

# Measurement of EEG Lead Fields Using Current Density Imaging with MRI?

M.L.G. Joy<sup>1\*</sup>, M. Kusano<sup>1</sup> & R.M. Henkelman<sup>2</sup>

1) Institute of Biomaterials and Biomedical Engineering & Department of Electrical and Computer Engineering. 2) Sunnybrook Health Science Center and Department of Medical Biophysics. University of Toronto, Toronto, Ontario, Canada. \* Presenter, mike.joy@utoronto.ca

**Abstract** We have developed a technique, Current Density Imaging (CDI), that allows electric currents to be imaged with clinical Magnetic Resonance Imagers. The method has been used in rabbits to image bipolar 40ms current pulses. It has also been used to image Radio Frequency (RF) currents in phantoms and the human leg. A possible application of these methods would be to measure the lead fields of EEG electrodes. Our hypothesis is that solutions of the inverse problem of the EEG, based on lead fields measured directly by CDI, will be more accurate than those based on a head model constructed using assumed tissue conductivities and simplified geometry.

We will support this hypothesis by showing CD images of rabbits which demonstrate the significant effect of the CSF on current pathways in the brain and the current signal to noise ratios which are achievable with CDI. We will show how RF CDI technique could be used to gather 20 lead fields in one hour of imaging. We will also describe work in progress on an electrically accurate MR head phantom with which we plan to test our hypothesis.

- The inverse problem of the EEG means finding bioelectric sources from scalp potentials.
- Assumed tissue conductivities means conductivity measurements made on one individual that are assumed to apply to another.

**Measured Lead Fields:** The linear relationship between bioelectric sources and measured potentials is:

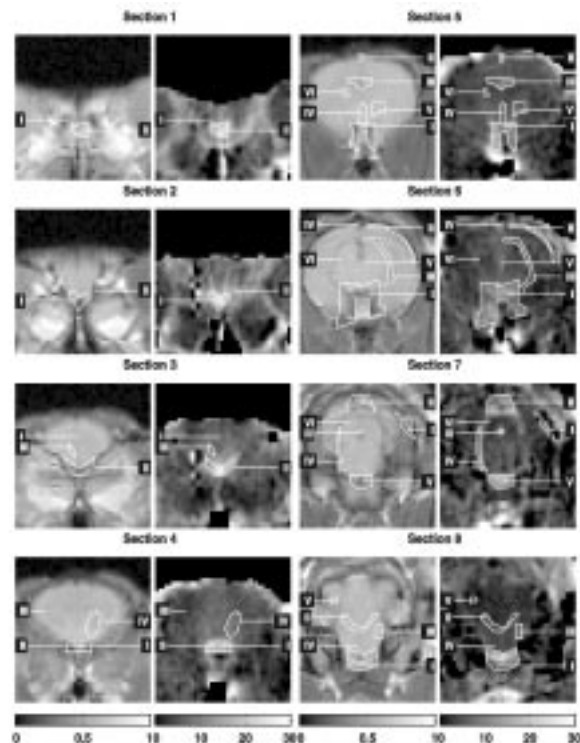
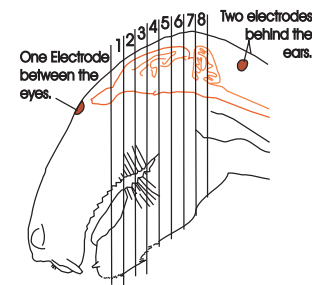
$$Az = u$$

where  $u$  is a vector of measured skin potentials,  $z$  is a longer vector of source dipole moments at points in the brain, and  $A$  is a matrix of forward transmission coefficients. The lead fields are the rows of matrix  $A$ . Row 1 defines how the potential measured by lead 1 depends upon the sources. The coefficients of row 1 are multiplied by the source dipole moments and summed to get the potential of lead 1. In 1969 Rush and Driscoll pointed out that, physically, these lead fields corresponded to either the current density (for voltage sources,  $E_s$ ) or the electric field intensity (for current sources,  $J_s$ ) produced at each source point when a unit current is applied between the lead and the reference electrode. They also prove that this result applies to *anisotropic* volume conductors. Lead fields are usually computed from the head model, however, we show that, when the lead fields are current densities, they can be directly imaged rather than computed.

The CD images shown on the right, after normalization by 19mA, are one component of the lead field for the electrode between the eyes with respect to the two behind the ears. Note that they do not resemble the lead fields computed from a head model with multiple shells. The CSF spaces clearly form pathways for current flow.

**Current Density Imaging:** The images below are of a live rabbit and made using a GE Signa 1.5T MR imager. Eight coronal slices, oriented as shown in the diagram, are shown. This diagram also shows

the position of the electrodes used to apply a current, with a peak value of 19mA, through the rabbit's head. For each slice two images are shown in the collage below. The image on the left is a normal MR image and that on the right is a CD image which shows the current flowing through the slice. Since these two images are made from the same MR dataset they are in exact register. Note that although both show the same anatomy, there is a marked difference between the two images.



**Section 1:** I-Olfactory bulb; II-Space between bulbs.

**Section 2:** I-Longitudinal fissure; II-Rhinal fissure.

**Section 3:** I-Longitudinal fissure; II-Ventro-lateral surface, Basal cisterna; III-Lateral ventricle.

**Section 4:** I-Chiasma; II-Chiasmatic cisterna; III-Centrum semiovale, IV-Lateral ventricle.

**Section 5:** I-Basal cisterna; II-Longitudinal fissure; III-Region of dorsal part of Third ventricle; IV-Ventral recess of Third ventricle; V-Space below pallium.

**Section 6:** I Cisterna interpeduncularis; II-Dorso-lateral cortex; III-Space around brain stem; IV-Longitudinal fissure; V-Third ventricle; VI-Thalamus.

**Section 7:** I-Dorso-lateral cortex; II-Region above colliculi; III-Aqueduct; IV-Space around midbrain; V-Cisterna pontis; VI-Periaqueductal grey.

**Section 8:** I-Basal cisterna; II-Fourth ventricle; III-Lateral recess of Fourth ventricle; IV-Reticular formation; V-Cerebellar nuclei.

The CD scale is shown at the bottom of the figure, the whitest regions correspond to 20 A/mm<sup>2</sup> or more, the blackest, to 0 A/mm<sup>2</sup> or negative.